Evolution of Efimov States in 2n Halo Nuclei: *A general study*

Indranil Mazumdar

TUNL, Duke University, NC
&
Dept. of Nuclear & Atomic Physics,
Tata Institute of Fundamental Research,
Mumbai 400 005

Chiral Dynamics, 2012

Jefferson Lab

9th August, 2012

Plan of the talk

- *Introduction to Efimov Effect*
- *The three-body formalism*
- *Searching for Efimov states in 2n halo nuclei:*

  ^{14}Be, ^{19}B, ^{20}C, ^{22}C, ^{38}Mg, ^{32}Ne ***some results***

- *Summary and future scope*

Collaborators

- V.S. Bhasin *Delhi Univ.*
- V. Arora *Delhi Univ.*
- A.R.P. Rau *Louisiana State Univ.*

- *Phys. Rev. Lett. 99, 269202*
- *Nucl. Phys. A790, 257*
- *Phys. Rev. Lett. 97, 062503*
- *Phys. Rev. C69, 061301(R)*
- *Phys. Rev. C61, 051303(R)*
- *Phys. Rev. C56, R5*
- *Phys. Rev. C50 , R550*
- *Few Body Systems, 2009*
- *Pramana, 2010*
- *Phys. Lett. B (2011)*

Phys. Rep 212 (1992) J.M. Richard
Phys. Rep. 231 (1993) 151(Zhukov et al.)
Phys. Rep. 347 (2001) 373 (Nielsen et al.)
Prog. Part. Nucl. Phys. 47,517 (2001) (Brown)
Rev. Mod. Phys. 76,(2004) 215(Jensen et al.)
Phys. Rep. 428, (2006) 259(Braaten & Hammer)
Ann Rev. Nucl. Part. Sci. 45, 591(Hansen et al.)
Rev. Mod. Phys. 66 (1105)(K. Riisager)
Rev. Mod. Phys. 82 (2910) 1225 (C. Chin et al.)

Efimov Effect

" A three-body system can support infinite bound states when none of the three pairs are bound, or one or two pairs are barely bound."

V. Efimov, Phys. Lett. B 33, 563 (1970); Comments Nucl. Part. Phys. 19, 271 (1990), Amado & Noble, Phys. Lett. B 35, 25 (1971)

Universality:

Independent of the details of the 2-body interaction

Adjacent energy levels are related by $\frac{E_{N+1}}{E_N} = e^{-2\pi}$

Size of the Nth state is $R_{size} \sim r_0 e^{N\pi}$

The number of states decreases with increasing 2-body strength

Necessary Conditions:

- Low energy requirement
- Large scattering length

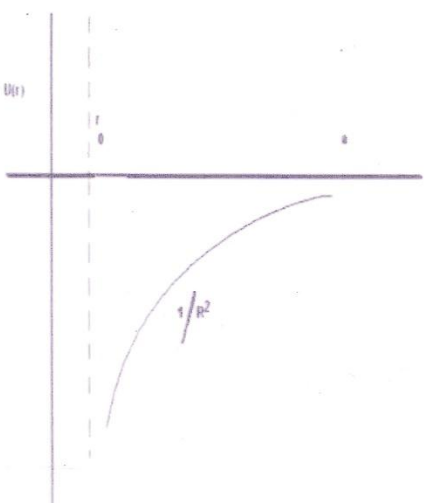

The Efimov Effect
(A Simple Visualisation)

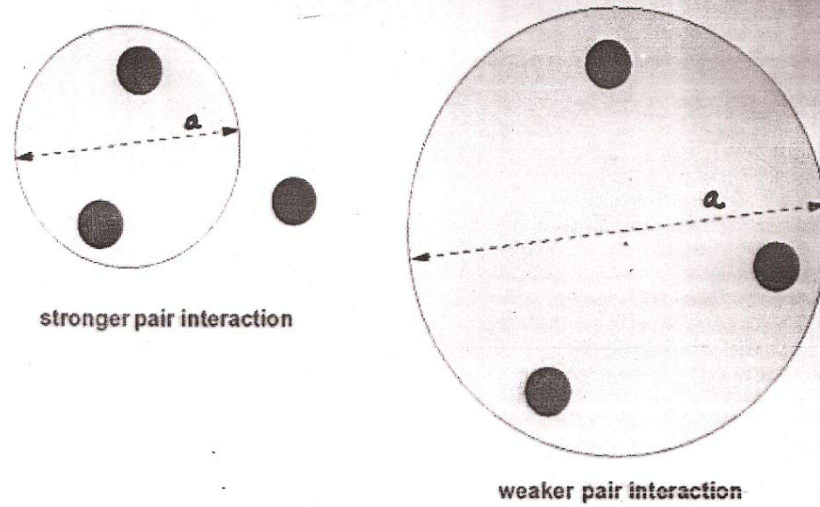

This scenario was predicted for three-body systems with

$a \gg r_0$	where	a = two-body scattering length r_0 = two-body effective range

Note: modern helium pair potentials have $a \approx 104$ Å, $r_0 \approx 11$ Å

Artificially weakening the pair interaction introduces up to infinitely many three-body bound states.

V. Efimov; Phys. Lett. **33B**, 563 (1970)

V. Efimov; Comments Nucl. Part. Phys. **19**, 271 (1990)

Efimov effect:

To
Efimov Physics

" From questionable to pathological to exotic to a hot topic ..."

Nature Physics 5, 533 (2009)

Vitaly Efimov
Univ. of Washington, Seattle

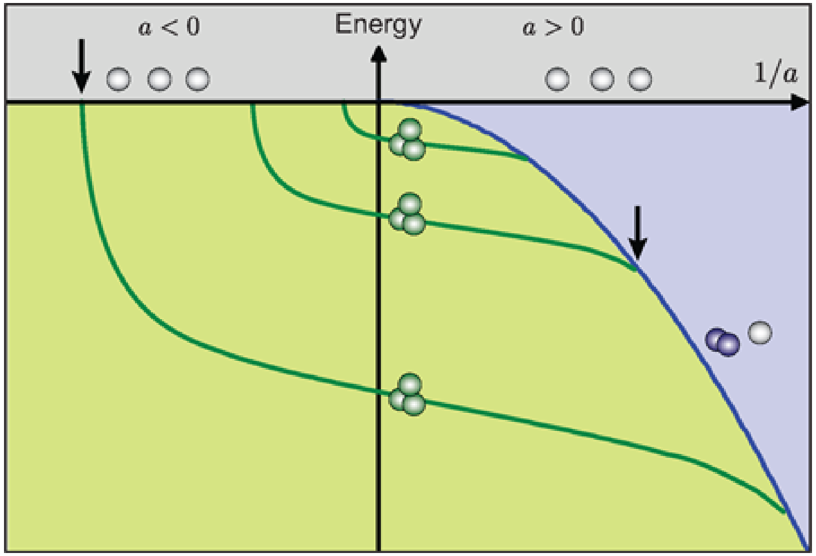

Efimov, 1990
Ferlaino & Grimm 2010

V. Efimov:
Sov. J. Nucl. Phys 12, 589 (1971)
Phys. Lett. 33B (1970)
Nucl. Phys A 210 (1973)
Comments Nucl. Part. Phys.19 (1990)

Amado & Noble:
Phys. Lett. 33B (1971)
Phys. Rev. D5 (1972)

Fonseca *et al*.
***Nucl. PhysA320, (1979*)**

Adhikari & Fonseca
Phys. Rev D24 (1981)

L.H. Thomas,
Phys.Rev.47,903(1935)

Theoretical searches in Atomic Systems

T.K. Lim *et al*. PRL38 (1977)

Cornelius & Glockle, J. Chem Phys. 85 (1986)

T. Gonzalez-Lezana et al. PRL 82 (1999),

The case of He trimer

Diffraction experiments with transmission gratings

Carnal & Mlynek, PRL 66 (1991)
Hegerfeldt & Kohler, PRL 84, (2000)

Three-body recombination in ultra cold atoms

First Observation of Efimov States

Letter

Nature **440**, 315-318 (16 March 2006) |

Evidence for Efimov quantum states in an ultracold gas of caesium atoms

T. Kraemer, M. Mark, P. Waldburger, J. G. Danzl, C. Chin, B. Engeser, A. D. Lange, K. Pilch, A. Jaakkola, H.-C. Nägerl and R. Grimm

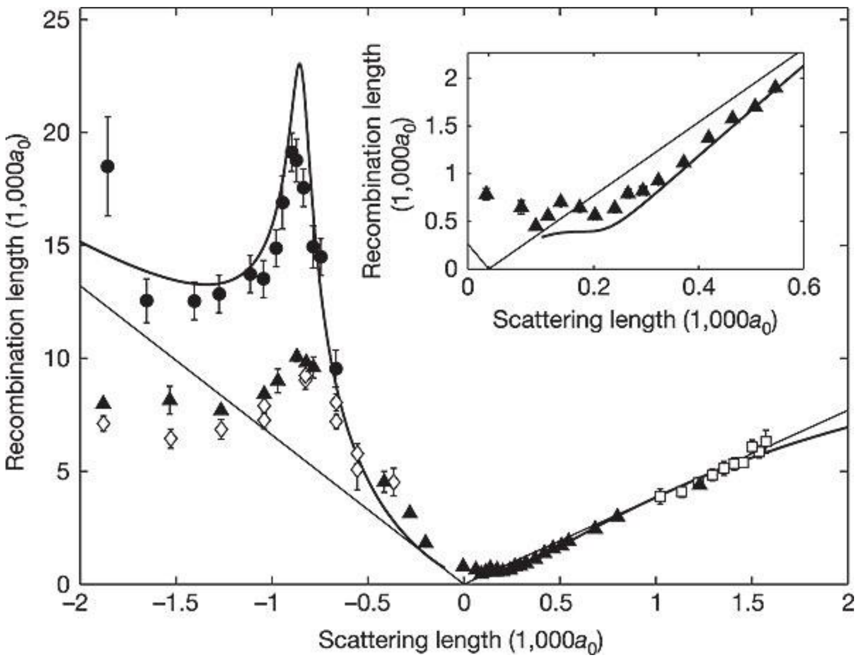

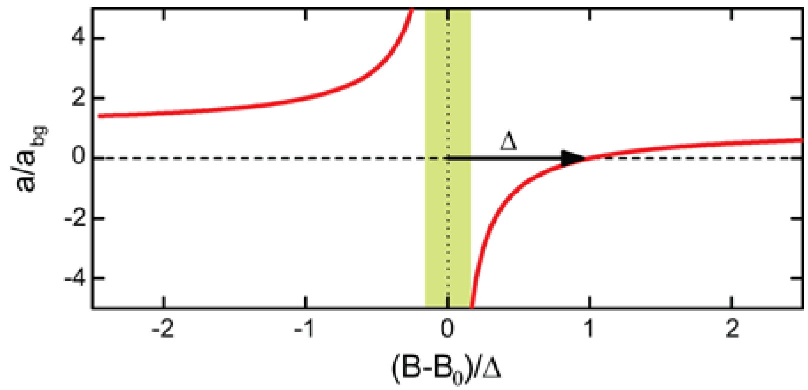

Observation of an Efimov spectrum in an atomic system.

M. Zaccanti et al. Nature Physics 5, 586 (2009)

First two states of the Efimovspectrum in ultra cold 39K

Can we find Efimov Effect in the atomic nucleus?

Unlike cold atom experiments we have no control over the scattering lengths.

The discovery of 2-neutron halo nuclei, characterized by very low separation energy and large spatial extension are ideally suited for studying Efimov effect in atomic nuclei.

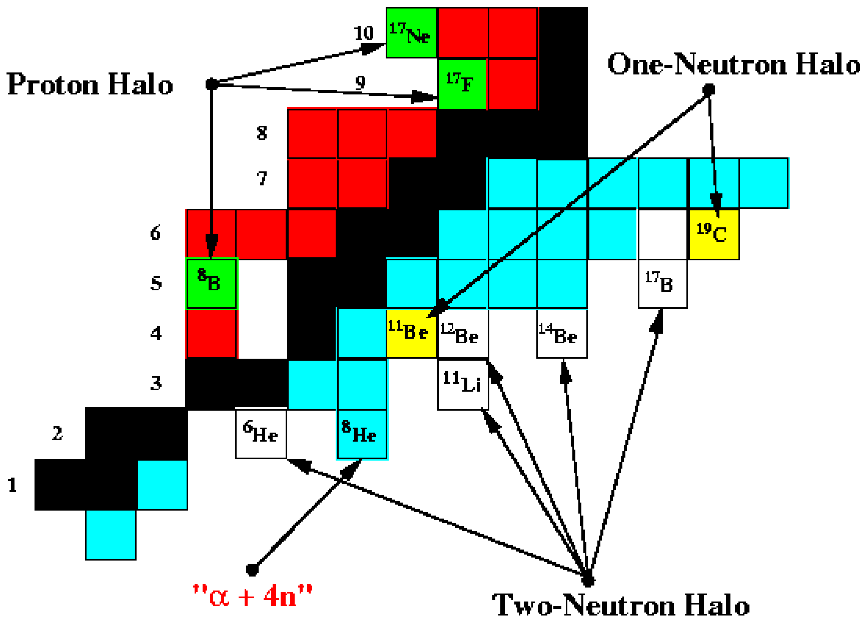

The Formalism

The 2-neutron halo nucleus ^{11}Li is modeled as a three-body system consisting of a compact core of ^{9}Li and two valence neutrons forming a halo around the core. We label the two neutrons and the core as 1,2,3 with momenta $\boldsymbol{P_1}$, $\boldsymbol{P_2}$, $\boldsymbol{P_3}$ respectively. Assuming the core to be a structureless and spinless object, we write the Schrodinger equation in momentum space as

$$(T - E)\psi = -(V_{12} + V_{23} + V_{31})\psi$$

Where E is the total energy (= - binding energy, B.E.) and T represents the kinetic energy such that

$$T - E = \boldsymbol{p}^2_1/2m + \boldsymbol{p}^2_2/2m + \boldsymbol{p}^2_3/2m_3 - E$$
$$= \boldsymbol{p}^2_{ij}/2\mu_{ij} + \boldsymbol{p}^2_k/2\mu_{ij\text{-}k} - E$$

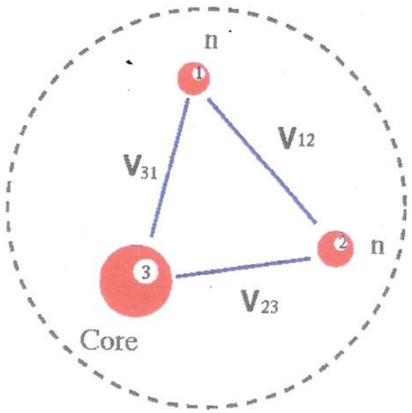

For the two-body interactions we consider non-local, separable potentials of the Yamaguchi form and assume *s*-state interactions both for n-n and n-^{9}Li systems.

The three body bound state wave function in momentum space using the binary separable potentials

$V_{12} = -\frac{\lambda_n}{2\mu_{12}} g(p_{12}) g(p'_{12})$,

$V_{23} = -\frac{\lambda_c}{2\mu_{23}} g(p_{23}) g(p'_{23})$,

$V_{31} = -\frac{\lambda_c}{2\mu_{31}} g(p_{31}) g(p'_{31})$ is

$$\psi(\vec{p}_{12}, \vec{p}_3; E) = D^{-1}(\vec{p}_{12}, \vec{p}_3; E)[g(p_{12})F(\vec{p}_3) + f(p_{23})G(\vec{p}_1) + f(p_{31})G(\vec{p}_2)] \quad (1)$$

$g(p) = 1/(p^2+\beta_n^2)$, $f(p)=1/(p^2+\beta_c^2)$, $\lambda_{n,c}$, $\beta_{n,c}$

reproduce spin singlet scattering length and effective range.

The spectator functions F(p) and G(p) satisfy the homogeneous coupled integral equations

$$[\Lambda_n^{-1} - h_n(p)]F(\vec{p}) = 2\int d\vec{q} K_1(\vec{p},\vec{q})G(\vec{q}) \quad (2)$$

$$[\Lambda_c^{-1} - h_c(p)]G(\vec{p}) = \int d\vec{q} K_2(\vec{p},\vec{q})F(\vec{q}) + \int d\vec{q} K_3(\vec{p},\vec{q})G(\vec{q}) \quad (3)$$

After the angular integration, the two couple equation reduce to an integral equation in one variable. These equations are numerically computed as an eigenvalue problem.

Dasgupta, Mazumdar, Bhasin, Phys. Rev C50,550

Structural properties of ^{11}Li

$$V_{12} = -\frac{\lambda_n}{2\mu_{12}} g(p_{12}) g(p'_{12}),$$

$$V_{23} = -\frac{\lambda_c}{2\mu_{23}} f(p_{23}) f(p'_{23}),$$

$$V_{31} = -\frac{\lambda_c}{2\mu_{31}} f(p_{31}) f(p'_{31}),$$

$$g(p) = 1/(p^2+\beta^2) \qquad \text{and} \qquad f(p) = 1/(p^2 + \beta_f^2).$$

Using the n-n and n-core potentials in the three-body Schrodinger equation,

$$(T\text{-}E)\psi = -(V_{12} + V_{23} + V_{31})\psi,$$

the solution (three-body wave function) is expressed as

$$\psi(\vec{p}_{12}, \vec{p}_{13}; E) = D^{-1}(\vec{p}_{12}, \vec{p}_3; E)[g(\vec{p}_{12})F(\vec{p}_3) + f(\vec{p}_{23})G(\vec{p}_1) + f(\vec{p}_{31})G(\vec{p}_2)], \tag{1}$$

where

$$D(\vec{p}_{12}, \vec{p}_3; E) \equiv \vec{p}_{12}^{\,2}/2\mu_{12} + \vec{p}_3^{\,2}/2\mu_{12,3} - E \tag{2}$$

The spectator functions $F(\vec{p})$ and $G(\vec{p})$ describe, respectively, the dynamics of the core and of the light halo particlessatisfy the homogeneous coupled integral equations

$$[\Lambda_n^{-1} - h_n(p)]F(\vec{p}) = 2\int d\vec{q} K_1(\vec{p}, \vec{q}) G(\vec{q}), \tag{3}$$

$$[\Lambda_c^{-1} - h_c(p)]G(\vec{p}) = \int d\vec{q} K_2(\vec{p}, \vec{q}) F(\vec{q}) + \int d\vec{q} K_3(\vec{p}, \vec{q}) G(\vec{q}), \tag{4}$$

where $\Lambda_n \equiv \lambda_n/2\mu_{12}$, $\Lambda_c \equiv \lambda_c/2\mu_{13}$. The explicit expressions for the kernels K_1, K_2 and K_3 are given by,

$$K_1(\vec{p}, \vec{q}; E) = \frac{m g(\vec{q} + \vec{p}/2) f(\vec{p} + a\vec{q})}{[q^2 + \vec{q}\cdot\vec{p} + p^2/2a - mE]}, \tag{5}$$

$$K_2(\vec{p}, \vec{q}; E) = \frac{m g(\vec{p} + \vec{q}/2) f(\vec{q} + a\vec{p})}{[p^2 + \vec{q}\cdot\vec{p} + q^2/2a - mE]}, \tag{6}$$

$$K_3(\vec{p}, \vec{q}; E) = \frac{m f(\vec{q} + b\vec{p}) f(\vec{p} + b\vec{q})}{[q^2/2a + \vec{q}\cdot\vec{p} + p^2/2a - mE]}, \tag{7}$$

with

$a \equiv m_3/(m+m_3)$, $b \equiv m/(m+m_3)$ and $d_3 \equiv (m+m_3)/(2m+m_3)$

$$h_n(p) = m\int d\vec{q} g^2(\vec{q})/[q^2 + p^2/2a - mE], \tag{8}$$

$$h_c(p) = m\int d\vec{q} f^2(\vec{q})/[q^2 + p^2/2d - mE]. \tag{9}$$

$\tau_n^{-1}(p)F(p) \equiv \phi(p)$ and $\tau_c^{-1}(p)G(p) \equiv \chi(p)$
Where

The basic structure of the equations in terms of the spectator functions F(p) and G(p) remains same. But for the sensitive computational details of the Efimov effect we recast the equations in dimensionless quantities.

$$\tau_n^{-1}(p) = \mu_n^{-1} - [\ \beta_r\ (\beta_r + \sqrt{p^2/2a + \varepsilon^3})^2\ ]^{-1}$$

$$\tau_c^{-1}(p) = \mu_c^{-1} - 2a[\ 1 + \sqrt{2a(p^2/4c + \varepsilon 3)}\ ]^{-2}$$

where $\mu_n = \pi^2\lambda_n/\beta_1^2$ and $\mu_c = \pi^2\lambda_c/2a\beta_1^3$

are the dimensionless strength parameters.
Variables *p* and *q* in the final integral equation are also now dimensionless,

$$p/\beta_1 \rightarrow p\ \&\ \ q/\beta_1 \rightarrow q$$

and

$$-mE/\beta_1^3 = \varepsilon_3,\ \ \beta_r = \beta/\beta_1$$

Factors τ_n^{-1} and τ_c^{-1} appear on the left hand side of the spectator functions F(p) and G(p) and are quite sensitive. They blow up as $p \rightarrow 0$ and ε_3 approaches extremely small value.

For our purpose of studying the sensitive computational details for the Efimov effect, the equations are suitably transformed in terms of ϕ(p) and χ(p), involving only the dimensionless quantities.

$$\tau_n^{-1}(p)F(p) \equiv \phi(p) \quad and \quad \tau_c^{-1}(p)G(p) \equiv \chi(p) \tag{1}$$

where τ_n^{-1}(p) = μ_n^{-1} - [$\beta_r(\beta_r + \sqrt{\frac{p^2}{2a} + \epsilon_3})^2]^{-1}$,

and τ_c^{-1}(p) = μ_c^{-1} - 2a[1+$\sqrt{2a(\frac{p^2}{4c} + \epsilon_3)}]^{-2}$,

with $\beta_r = \frac{\beta}{\beta_1}$, and μ_n= $\pi^2\lambda_n/\beta_1^3$ and μ_c= $\pi^2\lambda_c/2a\beta_1^3$ are the dimensionless strength parameters.

The two coupled equations are now reduced to one integral equation for χ(p)

$$\Lambda_i\chi(\vec{p}) = \int d\vec{q}K_3(\vec{p},\vec{q},\epsilon_3)\tau_c(\vec{q})\chi(\vec{q}) + 2\int d\vec{q}d\vec{q'}K_2(\vec{p},\vec{q},\epsilon_3)\tau_n(\vec{q}) \times K_1(\vec{q},\vec{q'},\epsilon_3)\tau_c(\vec{q'})\chi(\vec{q'}). \tag{2}$$

Here the kernels K_1, K_2, K_3 are essentially the same except that the variables p,q etc. are now dimensionless quantities: $\frac{p}{\beta_1} \to$ p, $\frac{q}{\beta_1} \to$ q, and $\frac{-mE}{\beta_1^2} \equiv \epsilon_3$.

The integral equation is basically an eigenvalue equation in Λ_i is computed numerically to determine the three-body (core-n-n) ground-state energy as well as the Efimov states. It is to be noted that the factors τ_n and τ_c are quite sensitive particularly when the scattering lengths of the binary systems get large values.

TABLE I. ^{14}Be ground and excited states three-body energy for different two-body input parameters.

n-^{12}Be Energy keV	λ1	a_s fm	ϵ_0 keV	ϵ_1 keV	ϵ_2 keV
50	11.71	−21	1350		
5.8	12.32	−61.6	1408	.053	
2	12.46	−105	1450	2.56	0.061
1	12.52	−149	1456	3.8	0.22
0.1	12.62	−483	1488	6.1	0.62
0.05	12.63	−658	1490	6.4	0.68
0.01	12.65	−1491	1490	6.9	0.72

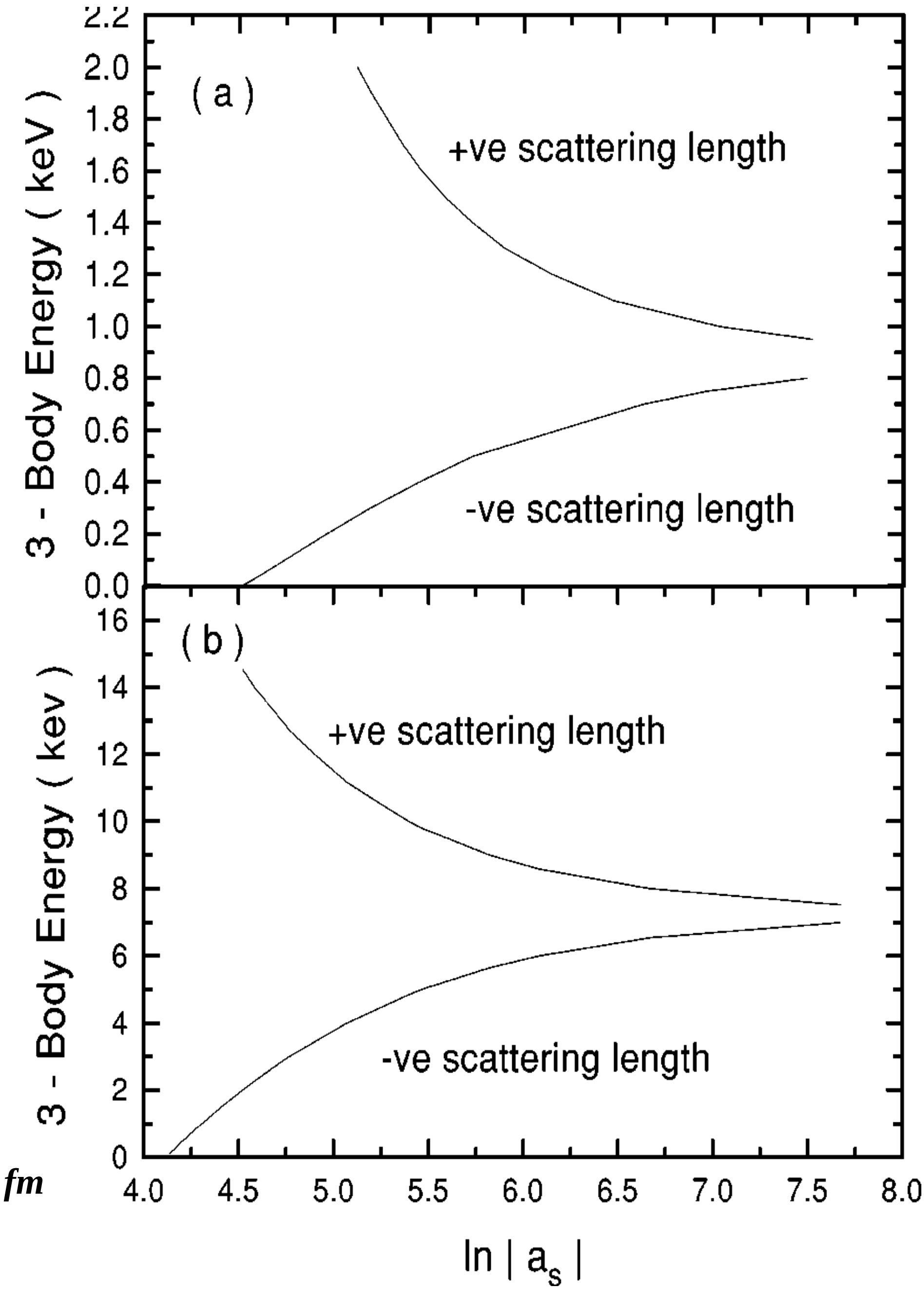

Mazumdar and Bhasin, PRC 56, R5

First Evidence for low lying s-wave strength in ^{13}Be

Fragmentation of ^{18}O, virtual state with scattering length < 10 fm

Thoennessen, Yokoyama, Hansen

Phys. Rev. C 63, 014308

Search for Efimov states in ^{19}B, ^{22}C, and ^{20}C

n-^{17}B energy (keV)	λ_c/α^3	a_s (fm)	ε_0 (keV)	ε_1 (keV)	ε_2 (keV)
514.8	8.49	-6.515	500		
135.3	9.5	-12.71	728		
48	10.0	-21.16	851		
7.7	10.5	-53.2	978	0.16	
0.67	10.75	-179.6	1042	5.4	0.36

n-^{20}C energy (keV)	λ_c/α^3	a_s (fm)	ε_0 (keV)	ε_1 (keV)	ε_2 (keV)
319	9.82	-8.23	1120		
127	10.5	-13.02	1287		
48.8	11.0	-21.0	1410		
9.3	11.5	-48.2	1540 0	0.122	
1.46	11.75	-121.5	1608	4.74	0.198

n-^{18}C energy (keV)	λ_c/α^3	a_s (fm)	ε_0 (keV)	ε_1 (keV)	ε_2 (keV)	
60	15.51	20.38	3188.03	78.87	65.8	1.01
100	15.89	16.05	3291.54	115.72	100.09	0.94
113.2	16.0	15.15	3317.35	127.41	111.76	0.92
139.60	16.2	13.77	3371.24	150.32	135.29	0.89
168.59	16.4	12.64	3426.03	175.34	163.48	0.86
200	16.6	11.71	3482.95	202.15	194.15	0.84

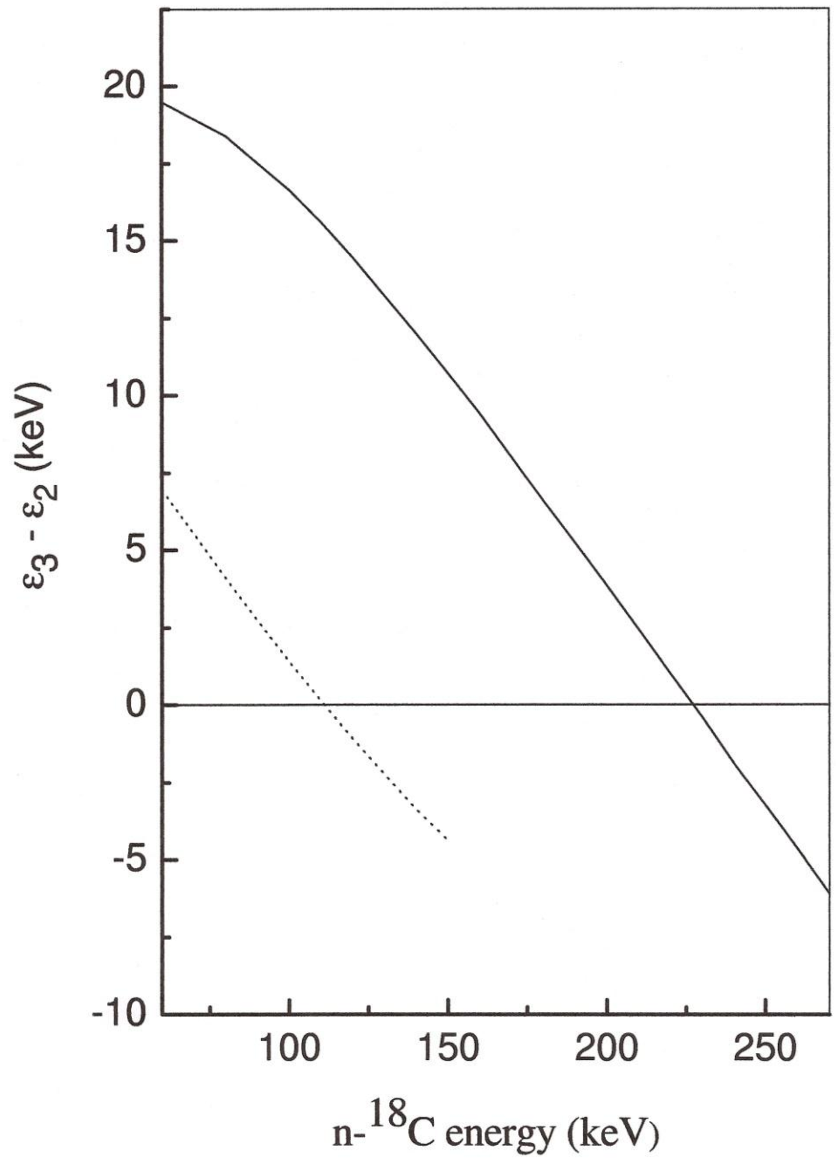

Mazumdar, Arora Bhasin
Phys. Rev. C 61, 051303(R)

Contents lists available at ScienceDirect

Physics Letters B

www.elsevier.com/locate/physletb

First evidence for a virtual ^{18}B ground state

A. Spyrou[a,b,*], T. Baumann[a], D. Bazin[a], G. Blanchon[c], A. Bonaccorso[d], E. Breitbach[e], J. Brown[f], G. Christian[a,b], A. DeLine[g], P.A. DeYoung[h], J.E. Finck[g], N. Frank[i], S. Mosby[a,b], W.A. Peters[j], A. Russel[g], A. Schiller[k], M.J. Strongman[a,b], M. Thoennessen[a,b]

dimensions, possibly of the order of 100 fm [1,10]. As shown by Mazumdar et al. [9], Efimov states would be expected in ^{19}B only if the unbound subsystem ^{18}B (n–^{17}B) would have a virtual ground state corresponding to a scattering length of a few hundred fm.

setup. An s-wave line shape was used to describe the experimental spectrum resulting in an upper limit for the scattering length of -50 fm which corresponds to a decay energy <10 keV. Observing an s-wave decay of ^{18}B provides an experimental verification that the ground state of ^{19}C includes a large s-wave component. The presence of this s-wave component shows that s–d mixing is still present in ^{18}B and that the $s_{1/2}$ orbital has not moved significantly below the $d_{5/2}$ orbital.

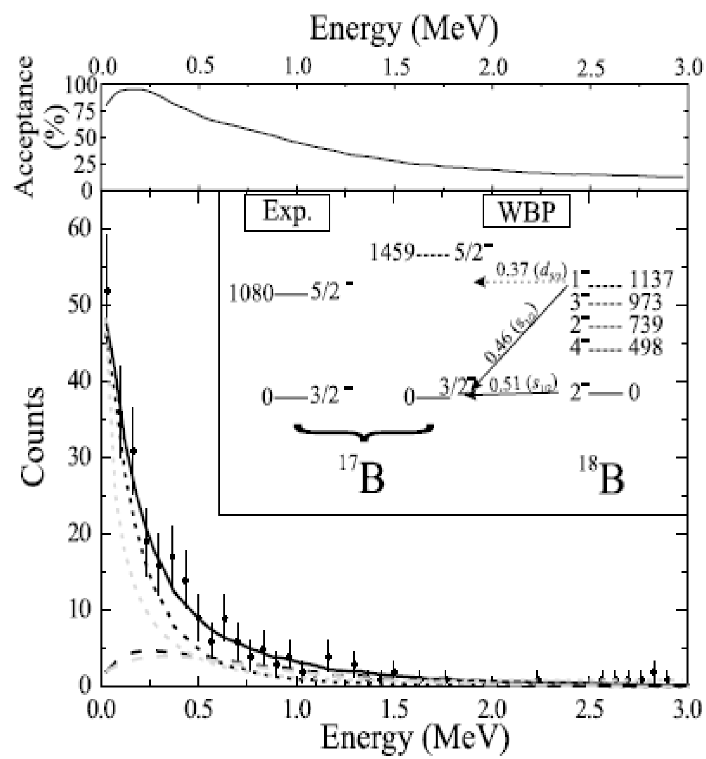

- *The feature observed can be attributed to the singularity in the two body propagator* $[\Lambda_C^{-1} - h_c(p)]^{-1}$.

- *There is a subtle interplay between the two and three body energies.*

- *The effect of this singularity on the behaviour of the scattering amplitude has to be studied.*

In order to analyze the effect of this singularity on the behavior of the scattering amplitude for n-^{19}C elastic scattering the function G(p) describing the dynamics of the neutron in the presence of (n-^{18}C) system, must be subject to the boundary condition, viz,

$$G(\vec{p}) = (2\pi)^3\delta(\vec{p}-\vec{k}) + \frac{4\pi a_k(\vec{p})}{p^2-k^2-\iota\epsilon} \quad (5)$$

The scattering amplitude is normalized such that, for the s-wave scattering,

$$a_k(\vec{p})_{|\vec{p}|=|\vec{k}|} \equiv f_k = \frac{e^{\iota\delta}sin\delta}{k} \quad (6)$$

Before applying the boundary condition, we rewrite Eq.(3) substituting Eq.(2) for F(p) and finally get the equation for the off-shell scattering amplitude as

$$4\pi(\frac{a}{d})h(p^2,k^2;\alpha_2^2)a_k(\vec{p}) =$$
$$(2\pi)^3K_3(\vec{p},\vec{k}) + 4\pi\int\frac{d\vec{q}K_3(\vec{p},\vec{q})a_k(\vec{q})}{q^2-k^2-\iota\epsilon} + (2\pi)^3\int d\vec{q}K_3(\vec{p},\vec{q})K_1(\vec{q},\vec{k})\tau_n(q) +$$
$$(8\pi)\int d\vec{q}K_3(\vec{p},\vec{q})\tau_n(q)\int d\vec{q'}\frac{K_1(\vec{q},\vec{q'})a_k(\vec{q'})}{q'^2-k^2-\iota\epsilon} \quad (7$$

This integral equation needs to be solved numerically for the scattering amplitude.

For k → 0, the singularity in the two body cut Does not cause any problem. The amplitude has only real part. The off-shell amplitude is computed By inverting the resultant matrix , which in the limit $a_o(p)_{p\to 0}$ → -a, the n-^{19}C scattering length.

For non-zero incident energies the singularity in the two body propagator is tackled by the CSM.

P → $p_1e^{-i\phi}$ and q → $qe^{-i\phi}$

The unitary requirement is the Im(f^{-1}_k) = -k

Balslev & Combes (1971)
Matsui (1980)
Volkov et al.

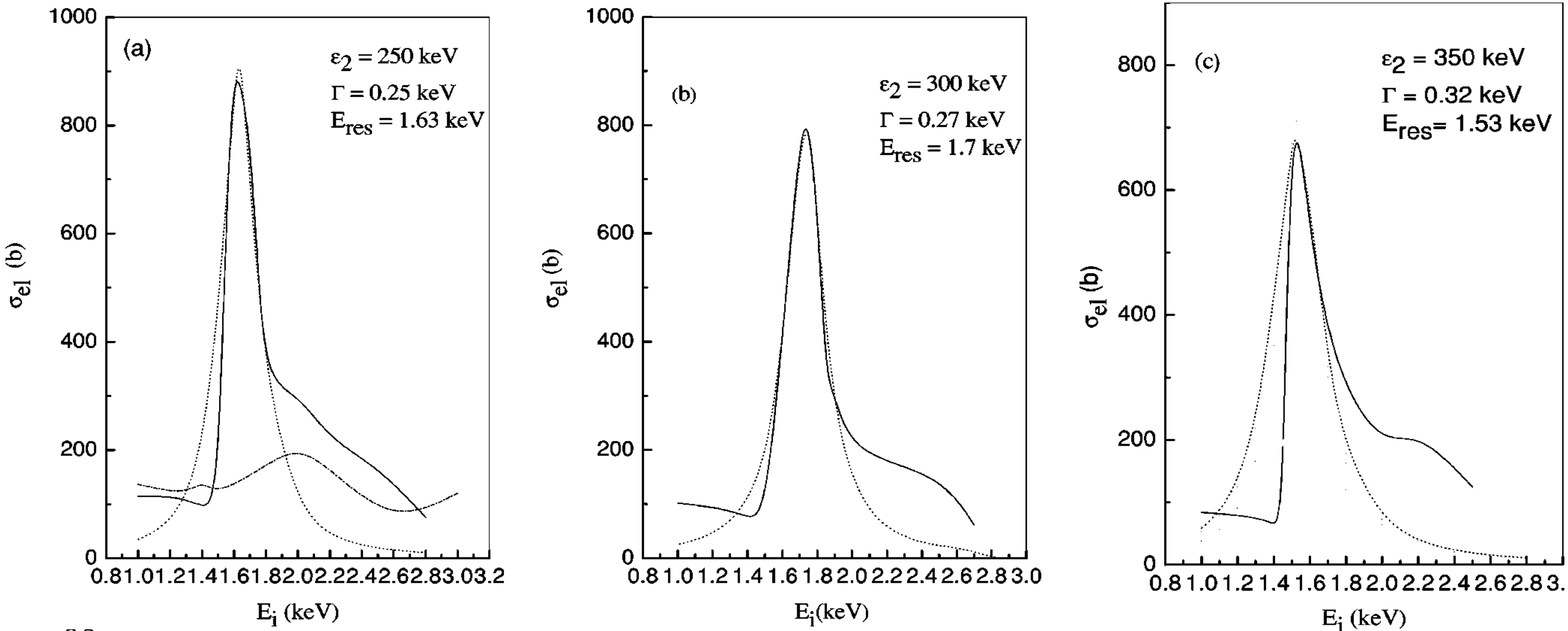

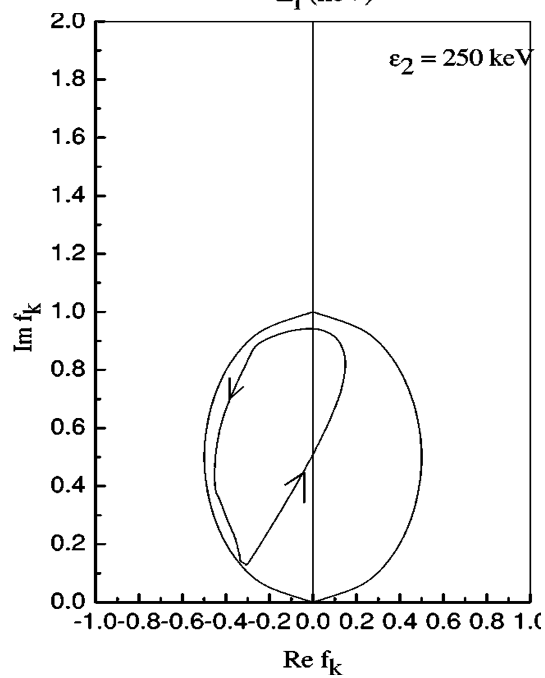

n-^{18}C Energy (keV)	$\varepsilon_3(0)$ (MeV)	$\varepsilon_3(1)$ (keV)	$\varepsilon_3(2)$ (keV)
60	3.00	79.5	66.95
100	3.10	116.6	101.4
140	3.18	152.0	137.5
180	3.25	186.6	-----
220	3.32	221.0	-----
240	3.35	238.1	-----
250	3.37	-----	-----
300	3.44	-----	-----

Arora, Mazumdar,Bhasin, PRC 69, 061301

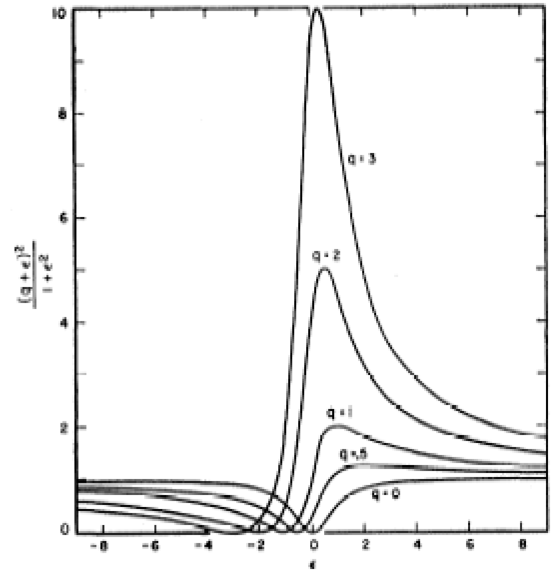

FIG. 1. Natural line shapes for different values of q. (Reverse the scale of abscissas for negative q.)

Ugo Fano

(1912 – 2001)

PHYSICAL REVIEW VOLUME 124, NUMBER 6 DECEMBER 15, 1961

Effects of Configuration Interaction on Intensities and Phase Shifts*

U. FANO
National Bureau of Standards, Washington, D. C.

(Received July 14, 1961)

Third highest in citation impact of all papers published in the entire Physical Review series.

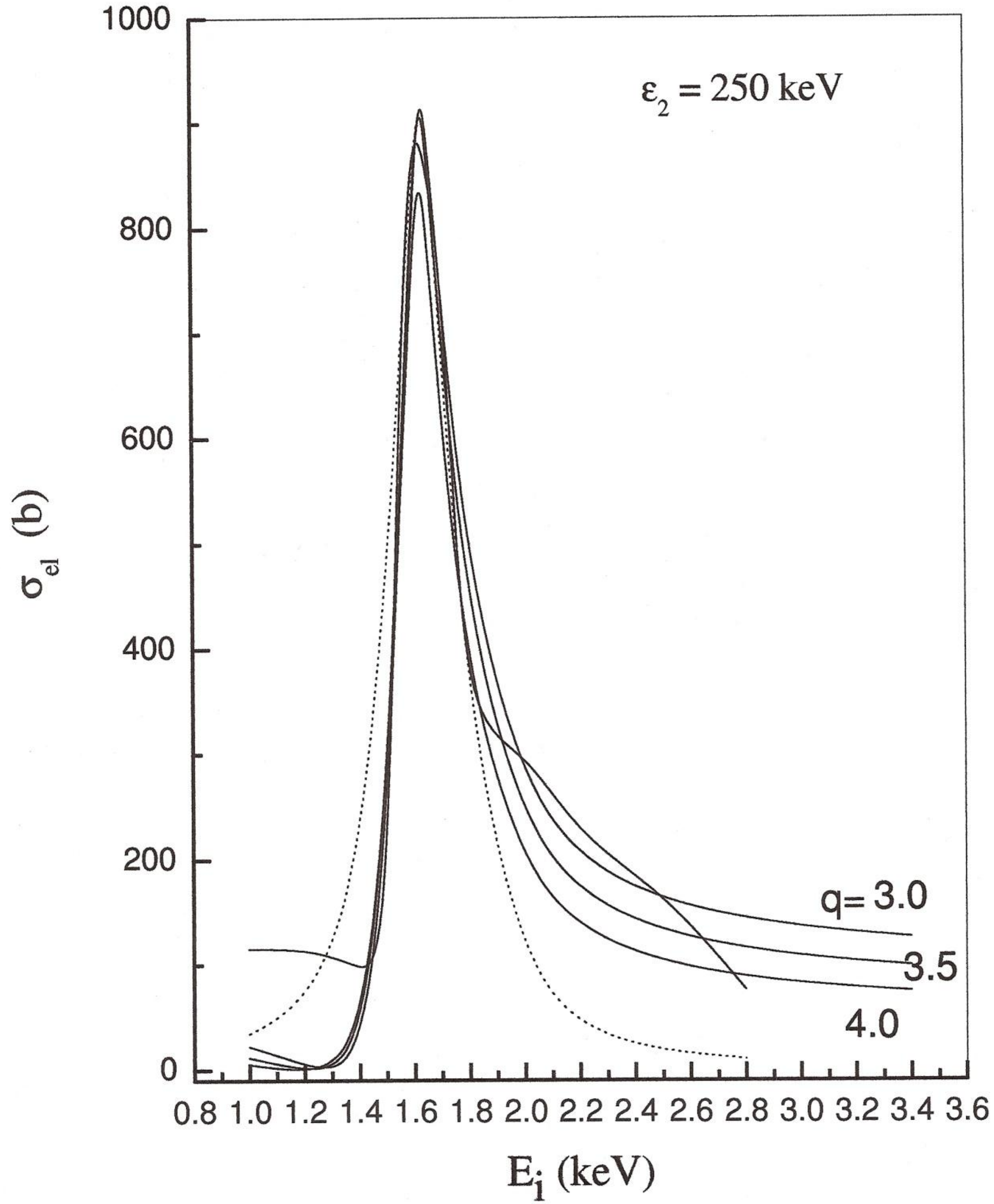

Fitting the Fano profile to the N-^{19}C elastic cross section for n-^{18}C BE of 250 keV

$$\sigma = \sigma_o[(q + \varepsilon)^2/(1+\varepsilon^2)]$$

Mazumdar, Rau, Bhasin
Phys. Rev. Lett. 97 (2006)

an ancient pond
a frog jumps in
a deep resonance

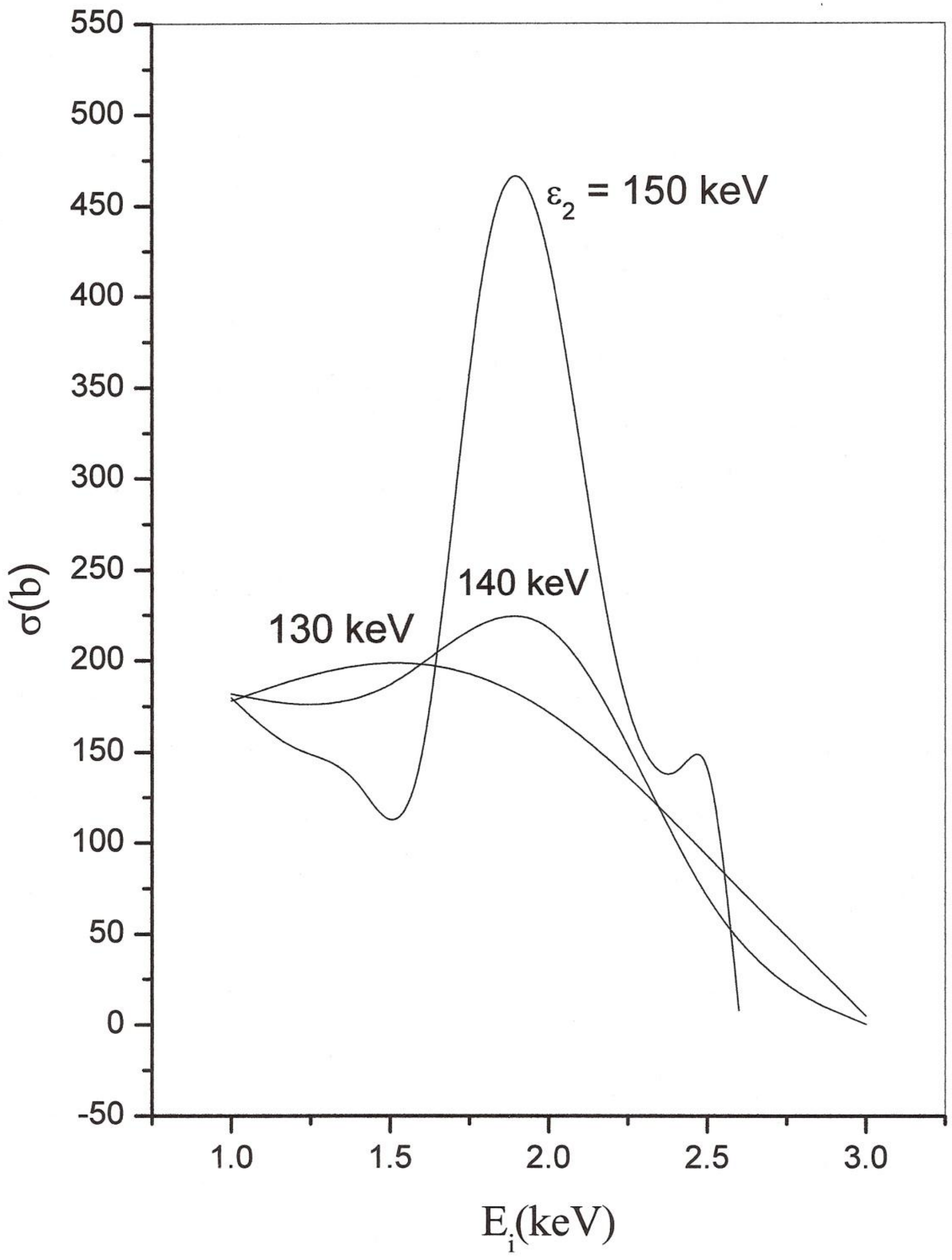

The resonance due to the second excited Efimov state for n-^{18}C BE 150 keV. The profile is fitted by same value of *q* as for the 250 keV curve.

The calculation have been extended to

1) Two hypothetical cases: ***very heavy core of mass A = 100 (+ 2n)***
three equal masses $m_1=m_2=m_3$

2) Two realistic cases of <u>^{38}Mg & ^{32}Ne</u>

Mazumdar, Bhasin, Rau
Phys. Lett. B 704, (2011)

^{38}Mg S_{2n} = 2570 keV n + core (^{37}Mg) 250 keV (bound)
^{32}Ne S_{2n} = 1970 keV n + core (^{31}Ne) 330 keV (bound)

^{38}Mg (S_{2n}) Audi & Wapstra (2003)

^{37}Mg & ^{31}Ne (S_n) Sakurai *et al*., PRC 54 (1996),
Jurado *et al.* PLB (2007), Nakamura *et al.* PRL (2009),

Hamamoto PRC (2010),
Urata, Hagino, Sagawa PRC (2011)

We have reproduced the ground state energies and have found at least two Efimov states that vanish into the continuum with increasing n-core interaction. They again show up as asymmetric resonances at around 1.6 keV neutron incident energy in the scattering sector.

TABLE: Ground and excited states for three cases studied, namely, mass 102 (columns 2, 3, 4), ^{38}Mg (column 5, 6, 7), and ^{32}Ne (columns 8, 9, 10) for different two body input parameters.

	^{102}A			^{38}Mg			^{32}Ne		
n-Core Energy ε_2 keV	$\varepsilon_3(0)$ keV	$\varepsilon_3(1)$ keV	$\varepsilon_3(2)$ keV	$\varepsilon_3(0)$ keV	$\varepsilon_3(1)$ keV	$\varepsilon_3(2)$ keV	$\varepsilon_3(0)$ keV	$\varepsilon_3(1)$ keV	$\varepsilon_3(2)$ keV
40	4020	53.6	44.4	3550	61.3	49.9	3420	61.5	50
60	4080	70.4	61.7	3610	80.8	67.1	3480	81.0	67.2
80	4130	86.9	(78.4)	3670	99.2	84.16	3530	99.8	84.3
100	4170	103.1		3710	117	101.4	3570	117.5	101.5
120	4220	(119.3)		3750	134.5	(118.9)	3620	135	(118.9)
140	4259			3790	151.6		3650	152.5	
180	4345			3860	185.6		3730	186.5	
250	4460			3980			3852		
300	4530			4040			3910		
350	4590			4120			3980		

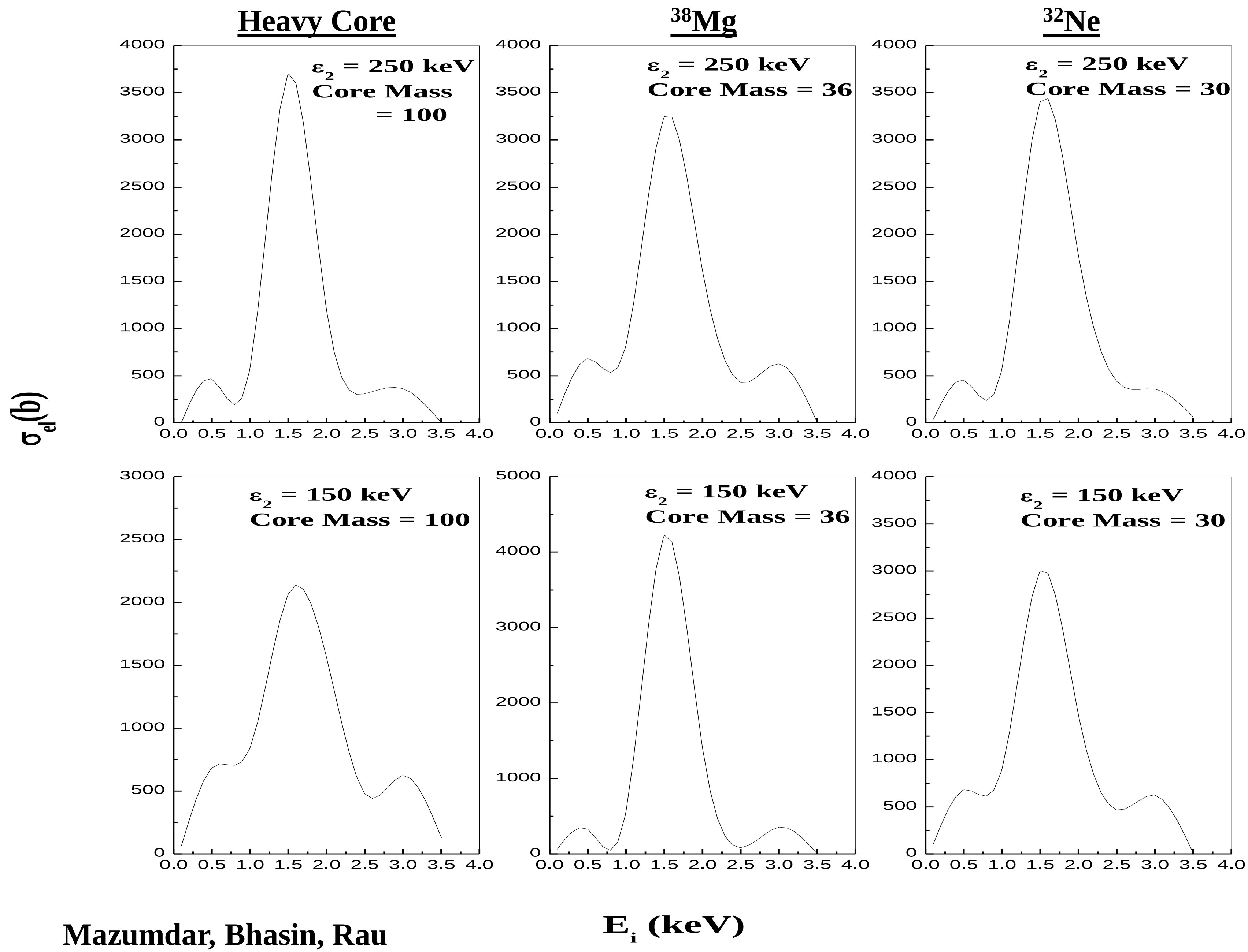

Mazumdar, Bhasin, Rau
Phys. Lett. B 704 (2011)

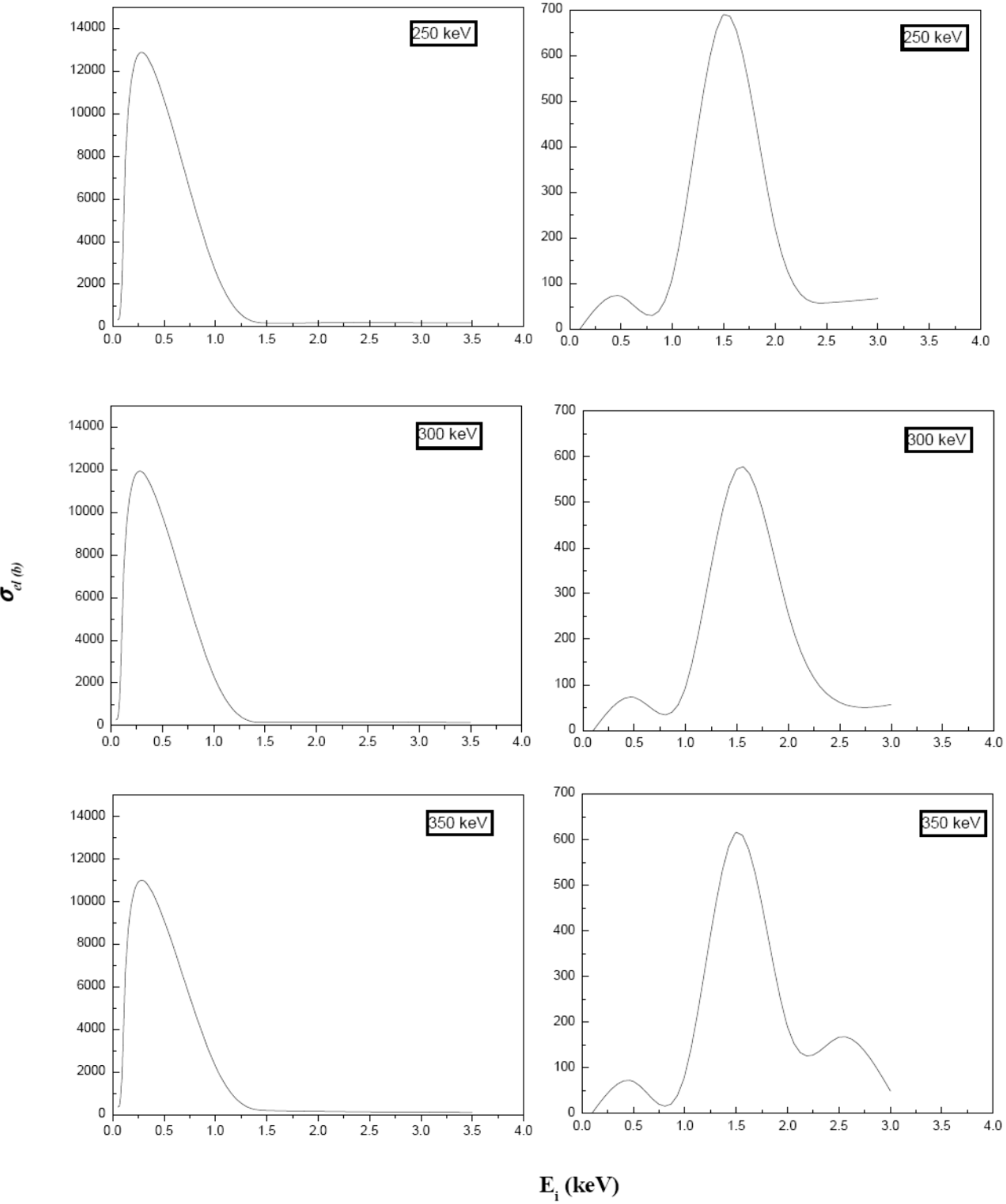

ε_o	Equal	Heavy Core
(keV)	(keV)	(keV)
250	455	4400
300	546	4470
350	637	4550

Ground states for the two cases

- ***Equal mass case strikingly different from unequal (heavy core) case.***
- ***Evolution of Efimov states in heavy core of 100 fully consistent with ^{20}C results.***

Mazumdar
Few Body Systems, 2009

Summary

- **A three body model with s-state interactions is exploited to search for Efimov states in 2n-halo nuclei.**

- **A virtual state of a few keV (2 to 4) energy corresponding to scattering length from -50 to -100 fm for the n-^{12}Be predicts the ground state and excited states of ^{14}Be.**

- **^{19}B, ^{22}C and ^{20}C are investigated and it is shown that Borromean type nuclei are much less vulnerable to respond to Efimov effect**

- **^{20}C is a promising candidate for Efimov states at energies below the n-(nc) breakup threshold.**

- ***The bound Efimov states in ^{20}C move into the continuum and reappear as Resonances with increasing strength of the binary interaction.***

- ***Asymmetric resonances in elastic n+^{19}C scattering are attributed to Efimov states and are identified with the Fano profile. The conjunction of Efimov and Fano phenomena may lead to the experimental realization in nuclei*.**

- ^{32}Ne & ^{38}Mg exhibit very similar dynamical structure and are also candidates for probing Efimov states.

- **We emphasize the cardinal role of channel coupling.**

  There is also a definite role of mass ratios as observed numerically.

- **However, channel coupling is an elegant and physically plausible scenario.**

- **Difference can arrive between zero range and realistic finite range potentials in non-Borromean cases.**

  Note, that for n-^{18}C binding energy of 200 keV, the scattering length is about 10 fm while the interaction range is about 1 fm.

- **The extension of zero range to finer details of Efimov states in non-Borromean cases may not be valid.**

- ***The discrepancy observed in the resonance vs virtual states in ^{20}C clearly underlines the sensitive structure of the three-body scattering amplitude derived from the binary interactions.***

Present Activities:

- Resonant states above the three body breakup threshold in ^{20}C.
- Structure calculations for ^{12}Be & ^{14}Be
- Role of Efimov states in Bose-Einstein condensation.
- Studying the proton halo (^{17}Ne) nucleus.
- **Planning for possible experiments with ^{20}C beam**

Epilogue

“ the richness of undestanding reveals even greater richness of ignorance”

D.H. Wilkinson

THANK YOU

Theoretical Models

- Shell Model *Bertsch et al. (1990) PRC 41,42,*
  Kuo et al. PRL 78,2708 (1997) 2 frequency shell model
  Brown (Prog. Part. Nucl. Physics 47 (2001)

Talmi & Unna, PRL 4, 496 (1960) ^{11}Be

S_n = 820 keV

S_n = 504 keV

Audi & Wapstra (2003)

Ab initio no-core full configuration calculation of light nuclei

Navratil, Vary, Barrett PRL84(2000), PRL87(2001)

Quantum Monte Carlo Calculations of Light Nuclei: ^{4,6,8}He, ^{6,7}Li, ^{8,9,10}Be

Pieper, Wiringa

- Cluster model

- Three-body model (for 2n halo nuclei)

- RMF model

- EFT *Braaten & Hammer, Phys. Rep. 428 (2006)*

- System composed of ultra-cold potassium atoms (^{39}K) with resonantly tunable two-body interaction.

- Atom-dimer resonance and loss mechanism

- Large values of *a* up to 25,000 a_o reached.

- First two states of an Efimov spectrum seen

Fedorov & Jensen
PRL 71 (1993)

Fedorov, Jensen, Riisager
PRL 73 (1994)

Conditions for occurrence of Efimov states in 2-n halo nuclei.

P. Descouvement
PRC 52 (1995), Phys. Lett. B331 (1994)

Striking Features:

- Extremely small separation energy S_n or S_{2n}
- Very large matter radius
- Narrow momentum distribution of fragments
- Borromean property of many two neutron halos(^{6}He, ^{11}Li, ^{14}Be)

Structure	Nucleus	S_n(kev)	S_{2n}(keV)
1n-halo	^{11}Be	504 ± 6	7317 ± 6
	^{19}C	160 ± 120	4350 ± 110
2n-halo	^{6}He	1864 ± 1	974 ± 1
	^{11}Li	330 ± 30	300 ± 30
	^{14}Be	1850 ± 120	1340 ± 110
	^{19}B	1030 ± 900	500 ± 430

S_{2n} = 369.15 (0.65) keV

Accepted lifetime:
8.80 (0.14) ms

$J^{\pi} = 3/2^{-}$

S_{2n} = 12.2 MeV for ^{18}O

Conditions for halo formation

- Small binding energy
- Small orbital angular momentum (most likely in s & p-state)
- Coulomb barrier hinders the formation of halo.
  (p-halos are less pronounced than n-halo)

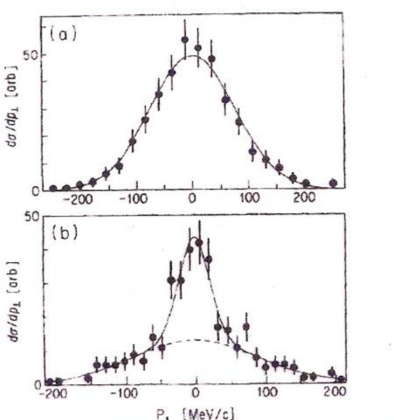

Typical experimental momentum distribution of halo nuclei from fragmentation reaction

Kobayashi *et al.*, PRL 60, 2599 (1988)

TABLE I. Parameters of the input two body (n-n and n-^{9}Li) potentials. Given the ^{11}Li binding energy, the strength parameter λ_c as obtained from the three-body equation is matched with the corresponding value obtained from the two-body analysis.

B.E. of ^{11}Li (MeV)	β/α	λ_n/α^3	β_1/α	λ_c/α^3	λ_c/α^3 three-body
0.34	5.8	18.6	5.0	10.32	12.92
	6.255	23.4	5.0	10.32	12.91
	5.8	18.6	5.5	14.0	17.01
0.20	5.8	18.6	5.0	10.32	12.39

TABLE II. Values of the root mean square radii of neutron-neutron and neutron-^{9}Li separations calculated using Eqs. (18) and (19) for different binding energies of ^{11}Li.

B.E. of ^{11}Li (MeV)	$\bar{r}_{nn}$ (fm)	$\bar{r}_{nn}$ (fm) (from other model calculations [4])	$\bar{r}_{nc}$ (fm)	$\bar{r}_{nc}$ (fm) (from other model calculations [4])
0.20	10.63		10.93	
0.25	9.9		9.86	
0.315	8.93	6.24 to 7.80	8.87	5.47 to 6.40

Dasgupta, Mazumdar, Bhasin
PRC50, R550

The rms radius r_{matter} calculated is ~ 3.6 fm

$$\langle r^2\rangle_{matter} = A_c/A\langle r^2\rangle_{core} + 1/A\langle \rho^2\rangle$$
$$\rho^2 = r^2_{nn} + r^2_{nc}$$

Fedorov et al (1993)
Garrido et al (2002) (3.2 fm)

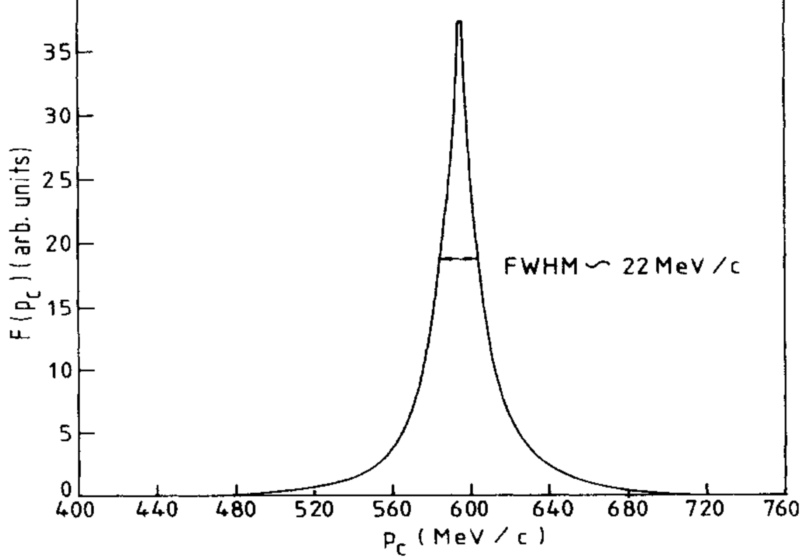

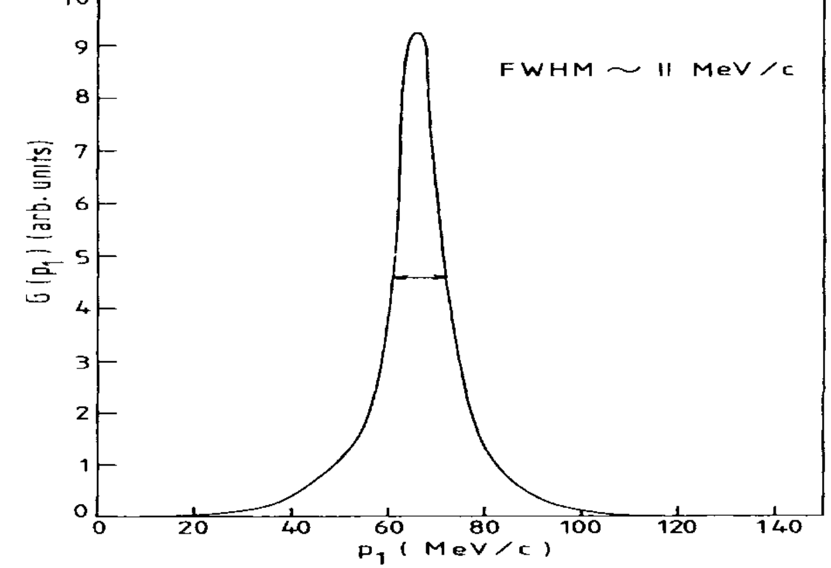

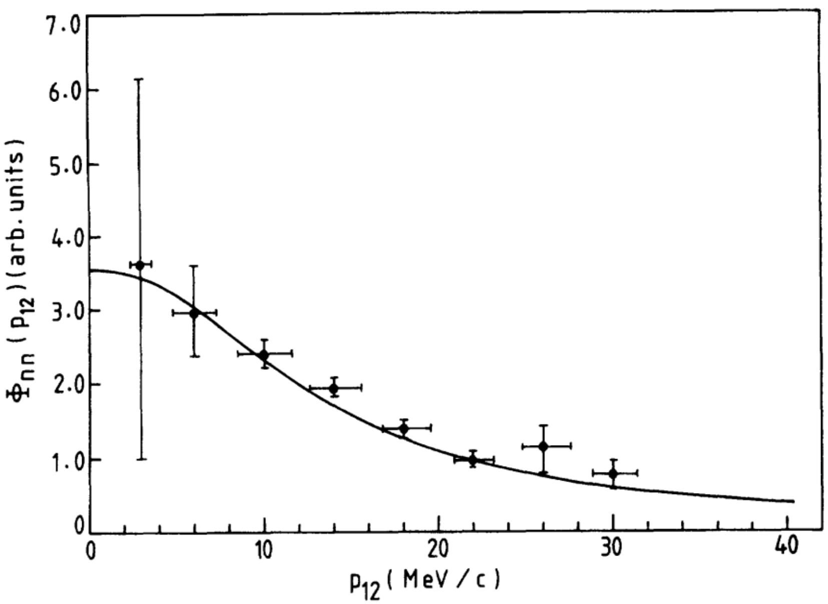

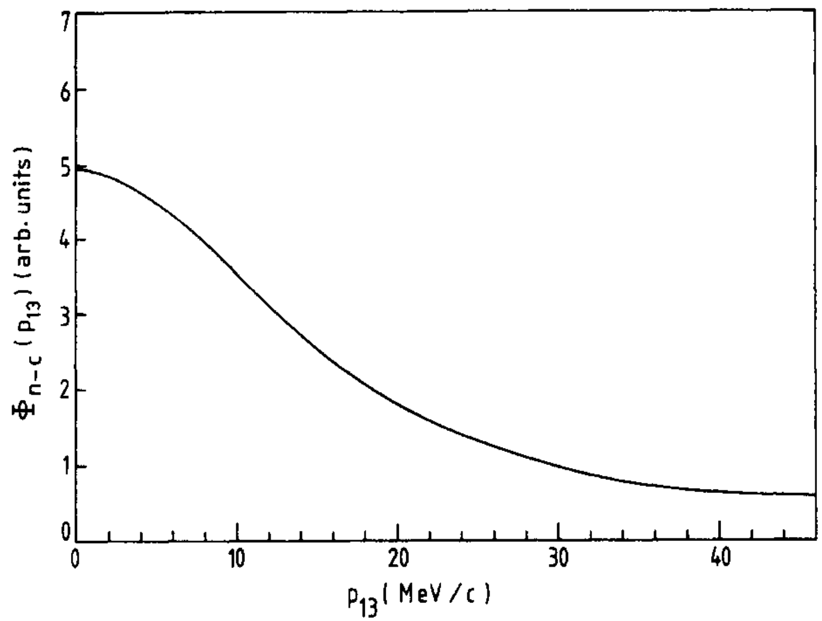

Dasgupta, Mazumdar, Bhasin, PRC 50, R550

Data:
Ieki et al,
PRL 70 ,1993

2-particle correlations:
Hagino et al , PRC, 2009

^{11}Li
Vs
^{6}He

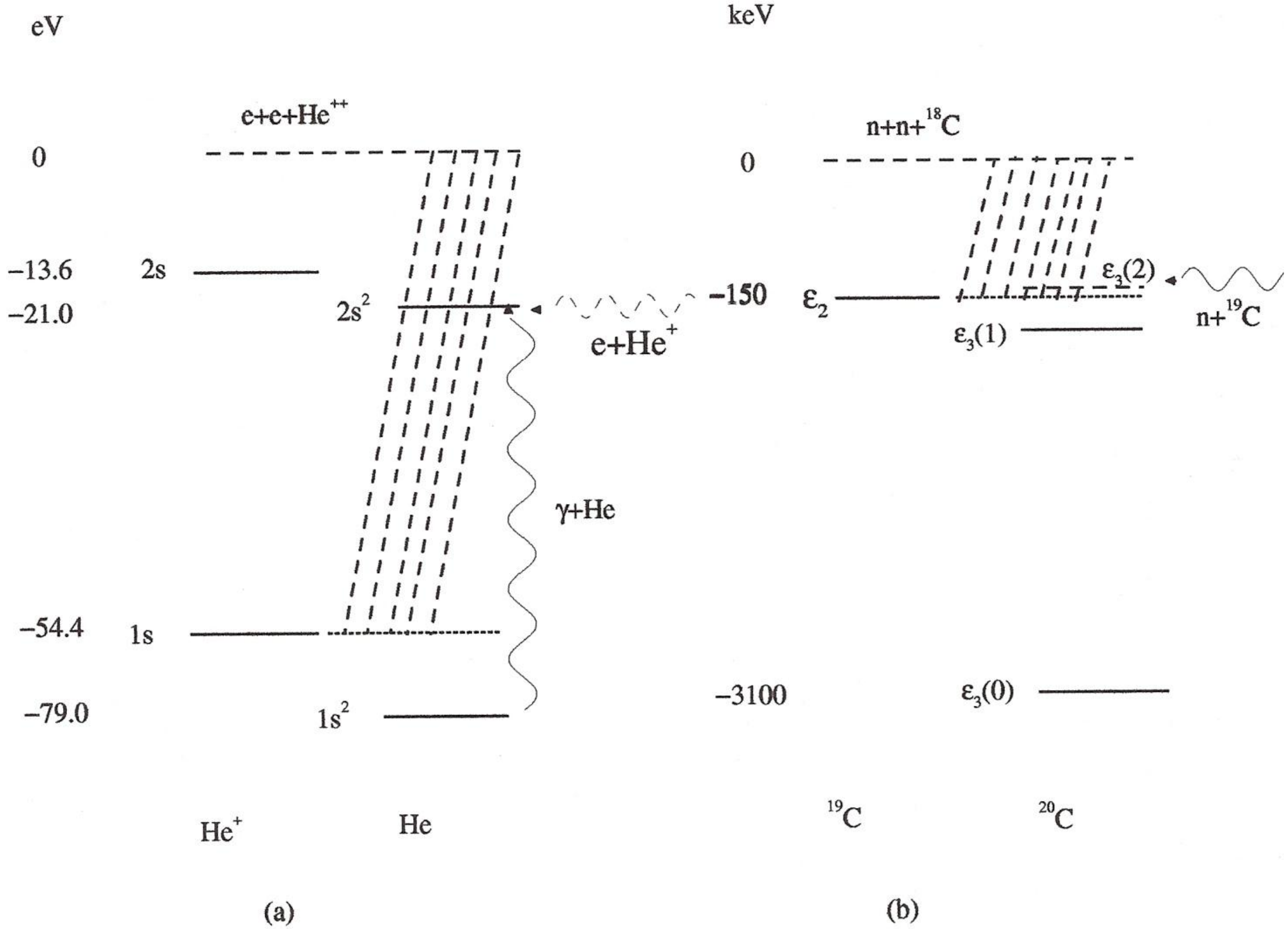

Comparison between He and ^{20}C as three body Systems in atoms and nuclei

Discussion

- **We emphasize the cardinal role of channel coupling.**

  There is also a definite role of mass ratios as observed numerically.

- **However, channel coupling is an elegant and physically plausible scenario.**

- **Difference can arrive between zero range and realistic finite range potentials in non-Borromean cases.**

  Note, that for n-^{18}C binding energy of 200 keV, the scattering length is about 10 fm while the interaction range is about 1 fm.

- **The extension of zero range to finer details of Efimov states in non-Borromean cases may not be valid.**

- ***The discrepancy observed in the resonance vs virtual states in ^{20}C clearly underlines the sensitive structure of the three-body scattering amplitude derived from the binary interactions.***

A possible experimental proposal to search for Efimov State in 2-neutron halo nuclei.

- **Production of ^{20}C secondary beam with reasonable flux**
- **Acceleration and Breakup of ^{20}C on heavy target**
- **Detection of the neutrons and the core in coincidence**
- **Measurement of γ-rays as well**

The Arsenal:

- ***Neutron detectors array***
- ***Gamma array***
- ***Charged particle array***

Another experimental scenario:

^{19}C beam on deuteron target:
Neutron stripping reaction

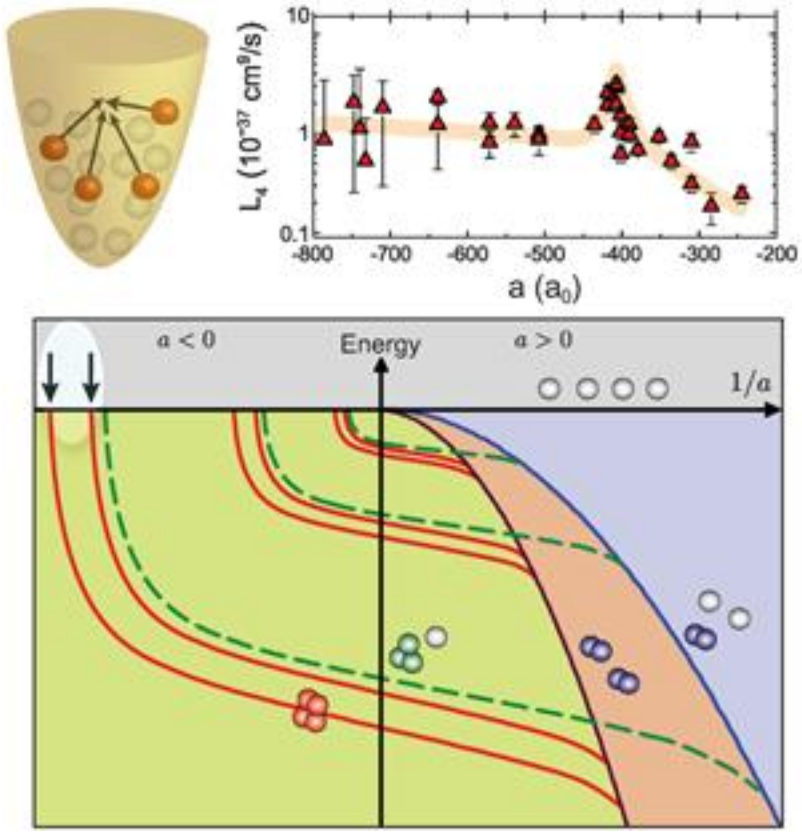

L_4 (10^{-37} cm^9/s)
10
1
0.1
-800
-700
-600
-500
-400
-300
-200
a (a_0)
$a < 0$
Energy
$a > 0$
$1/a$

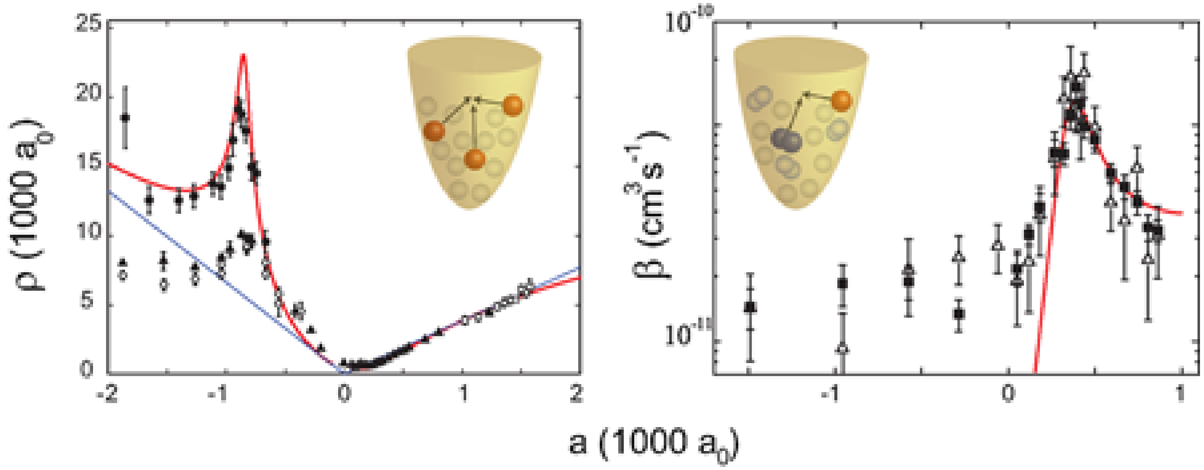

25
20
15
10
5
0
-2
-1
0
1
2
ρ (1000 a0)
10^-10
10^-11
-1
0
1
β (cm3 s-1)
a (1000 a0)

Appearance of Resonance in n-^{19}C Scattering

- The equation for the off-shell scattering amplitude in n-^{19}C (bound state of n-^{18}C) can be written as

$$4\pi\left(\frac{a}{d}\right)h(p^2,k^2;\alpha_2^2)a_k(\vec{p}) = (2\pi)^3 K_3(\vec{p},\vec{k}) + 4\pi\int \frac{d\vec{q}K_3(\vec{p},\vec{q})a_k(\vec{q})}{q^2-k^2-\iota\epsilon}$$

$$+2(2\pi)^3\int d\vec{q}K_2(\vec{p},\vec{q})K_1(\vec{q},\vec{k})\tau_n(q)$$

$$+2(4\pi)\int d\vec{q}K_2(\vec{p},\vec{q})\tau_n(q)\int d\vec{q}'\frac{K_1(\vec{q},\vec{q}')a_k(\vec{q}')}{q'^2-k^2-\iota\epsilon}.$$

- where a $_k$(p) is the off-shell scattering amplitude, normalized such that

$$a_k(\vec{p})_{|\vec{p}|=|\vec{k}|} = f_k = \frac{e^{\iota\delta}\sin\delta}{k}.$$